

 Open access • Journal Article • DOI:10.1063/1.4946841

Mixed-mode high-power impulse magnetron sputter deposition of tetrahedral amorphous carbon with pulse-length control of ionization — [Source link](#)

M. D. Tucker, R. Ganesan, Dougal G. McCulloch, Jim G. Partridge ...+5 more authors

Institutions: Curtin University, University of Sydney, RMIT University, Karlsruhe Institute of Technology

Published on: 21 Apr 2016 - Journal of Applied Physics (AIP Publishing)

Topics: High-power impulse magnetron sputtering, Amorphous carbon, Carbon film, Sputter deposition and Elastic recoil detection

Related papers:

- [A strategy for increased carbon ionization in magnetron sputtering discharges](#)
- [Exploring the potential of high power impulse magnetron sputtering for growth of diamond-like carbon films](#)
- [Diamond-like amorphous carbon](#)
- [Ionized physical vapor deposition \(IPVD\): A review of technology and applications](#)
- [Interpretation of Raman spectra of disordered and amorphous carbon](#)

Share this paper:    

View more about this paper here: <https://typeset.io/papers/mixed-mode-high-power-impulse-magnetron-sputter-deposition-5cnp5ix3uq>



Mixed-mode high-power impulse magnetron sputter deposition of tetrahedral amorphous carbon with pulse-length control of ionization

Tucker, M; Ganesan, R.; McCulloch, D; Partridge, J; Stueber, M; Ulrich, S; Bilek, M.

https://researchrepository.rmit.edu.au/discovery/delivery/61RMIT_INST:ResearchRepository/12247137900001341?l#13248373690001341

Tucker, Ganesan, R., McCulloch, D., Partridge, J., Stueber, M., Ulrich, S., Bilek, M., McKenzie, D., & Marks, N. (2016). Mixed-mode high-power impulse magnetron sputter deposition of tetrahedral amorphous carbon with pulse-length control of ionization. *Journal of Applied Physics*, 119(15), 1–6.

<https://doi.org/10.1063/1.4946841>

Document Version: Published Version

Published Version: <https://doi.org/10.1063/1.4946841>

Repository homepage: <https://researchrepository.rmit.edu.au>

© 2016 Author(s).

Downloaded On 2022/05/31 00:42:28 +1000



Thank you for downloading this document from the RMIT Research Repository.

The RMIT Research Repository is an open access database showcasing the research outputs of RMIT University researchers.

RMIT Research Repository: <http://researchbank.rmit.edu.au/>

Citation:

Tucker, M, Ganesan, R, McCulloch, D, Partridge, J, Stueber, M, Ulrich, S, Bilek, M, McKenzie, D and Marks, N 2016, 'Mixed-mode high-power impulse magnetron sputter deposition of tetrahedral amorphous carbon with pulse-length control of ionization', Journal of Applied Physics, vol. 119, no. 15, 155303, pp. 1-6.

See this record in the RMIT Research Repository at:

<https://researchbank.rmit.edu.au/view/rmit:36936>

Version: Published Version

Copyright Statement:

© 2016 Author(s).

Link to Published Version:

<https://dx.doi.org/10.1063/1.4946841>

PLEASE DO NOT REMOVE THIS PAGE

Mixed-mode high-power impulse magnetron sputter deposition of tetrahedral amorphous carbon with pulse-length control of ionization

Cite as: J. Appl. Phys. **119**, 155303 (2016); <https://doi.org/10.1063/1.4946841>

Submitted: 05 February 2016 . Accepted: 03 April 2016 . Published Online: 21 April 2016

M. D. Tucker, R. Ganesan, D. G. McCulloch, J. G. Partridge, M. Stueber, S. Ulrich, M. M. M. Bilek, D. R. McKenzie , and N. A. Marks



View Online



Export Citation



CrossMark

ARTICLES YOU MAY BE INTERESTED IN

[Tutorial: Reactive high power impulse magnetron sputtering \(R-HiPIMS\)](#)

Journal of Applied Physics **121**, 171101 (2017); <https://doi.org/10.1063/1.4978350>

[Synthesis of hydrogenated diamondlike carbon thin films using neon-acetylene based high power impulse magnetron sputtering discharges](#)

Journal of Vacuum Science & Technology A **34**, 061504 (2016); <https://doi.org/10.1116/1.4964749>

[Evolution of target condition in reactive HiPIMS as a function of duty cycle: An opportunity for refractive index grading](#)

Journal of Applied Physics **121**, 171909 (2017); <https://doi.org/10.1063/1.4977824>

Lock-in Amplifiers up to 600 MHz

starting at

\$6,210



 Zurich
Instruments

Watch the Video



Mixed-mode high-power impulse magnetron sputter deposition of tetrahedral amorphous carbon with pulse-length control of ionization

M. D. Tucker,¹ R. Ganesan,² D. G. McCulloch,³ J. G. Partridge,³ M. Stueber,⁴ S. Ulrich,⁴ M. M. M. Bilek,² D. R. McKenzie,² and N. A. Marks¹

¹Department of Physics and Astronomy, Curtin University, Perth, Western Australia 6102, Australia

²School of Physics, The University of Sydney, Sydney, New South Wales 2006, Australia

³School of Applied Sciences, RMIT University, GPO Box 2476, Melbourne, Victoria 3001, Australia

⁴Karlsruhe Institute of Technology—KIT, Institute for Applied Materials—IAM, Hermann-von-Helmholtz-Platz 1, 76344 Eggenstein-Leopoldshafen, Germany

(Received 5 February 2016; accepted 3 April 2016; published online 21 April 2016)

High-power impulse magnetron sputtering (HiPIMS) is used to deposit amorphous carbon thin films with sp^3 fractions of 13% to 82%. Increasing the pulse length results in a transition from conventional HiPIMS deposition to a “mixed-mode” in which an arc triggers on the target surface, resulting in a large flux of carbon ions. The films are characterized using X-ray photoelectron spectroscopy, Raman spectroscopy, ellipsometry, nanoindentation, elastic recoil detection analysis, and measurements of stress and contact angle. All properties vary in a consistent manner, showing a high tetrahedral character only for long pulses, demonstrating that mixed-mode deposition is the source of the high carbon ion flux. Varying the substrate bias reveals an “energy window” effect, where the sp^3 fraction of the films is greatest for a substrate bias around -100 V and decreases for higher or lower bias values. In the absence of bias, the films’ properties show little dependence on the pulse length, showing that energetic ions are the origin of the highly tetrahedral character.

Published by AIP Publishing. [<http://dx.doi.org/10.1063/1.4946841>]

I. INTRODUCTION

Amorphous carbon thin films have been extensively studied for decades and have found numerous technological applications.^{1,2} This interest is due to the possibility of controlling the proportions of sp^2 and sp^3 bonding as well as the flexibility afforded by a wide variety of deposition techniques including evaporation, sputtering, ion-beam deposition, cathodic arcs, and chemical vapour deposition. Tetrahedral amorphous carbon (*ta*-C) and hydrogenated *ta*-C (*ta*-C:H) are often desired due to their diamond-like properties, while in many industrial applications, amorphous carbon (*a*-C) and hydrogenated *a*-C (*a*-C:H) do an excellent job as well. This range of possibilities means that amorphous carbon coatings are found in applications ranging from the automotive industry, where tribological performance is important, to medical devices, where surface energies and wetting behaviour are of concern.

Carbon deposition sources that generate a high fraction of ions are particularly attractive as they offer control of the kinetic energy of the depositing flux. Energetic ions result in dense films, and even when the carbon ion fraction is minimal, such as in sputtering, it is possible to synthesize dense and hard amorphous carbon films by bombarding the growing film with argon ions, either by using a substrate bias³ or by using a separate Ar ion source.⁴ With a highly ionized carbon plasma, such as produced by cathodic arc deposition, laser ablation, or mass-selected ion beam deposition, optimal energies of ~ 100 eV produce tetrahedral amorphous carbon (*ta*-C) films with sp^3 fractions as high as 85%.^{5–7} There have also been many attempts to deposit *ta*-C using sputtering techniques,^{4,8,9} which are attractive due to their ubiquity in large-scale coating. However, these efforts are hindered by

the near absence of carbon ions in the sputtered flux of a conventional magnetron, limiting the ability to control the incident ion energy. High Power Impulse Magnetron Sputtering (HiPIMS)^{10–15} has been found to increase the ionized fraction when sputtering metals,¹⁶ but for carbon, the effect is small and the films remain predominantly sp^2 bonded.^{17–26}

We have recently demonstrated a new process in which HiPIMS sputtering is repeatedly driven into an arc mode.²⁷ Using this “mixed-mode,” we synthesized *ta*-C with an sp^3 fraction of 80% as shown by electron energy loss spectroscopy (EELS) and X-ray photoelectron spectroscopy (XPS).²⁸ The defining characteristic of mixed-mode operation is that the magnetron current increases to a degree such that an arc ignites on the surface of the carbon target.^{27,29} The arcs exhibit characteristics of carbon cathodic arcs including retrograde motion in a magnetic field, fractal-like branching of the arc spots, and a minimum average ion energy of 20 eV.²⁸ These arcs result in increased ionization in the depositing flux and are the means by which the high sp^3 fraction of the films is obtained. Deposition of *ta*-C films required Ar pressures of 0.3 Pa or lower. At higher pressures, all the measures of the tetrahedral character of the films deteriorated, presumably due to a decreased ion flux at the substrate caused by charge-exchange scattering with Ar neutrals.

In this article, we explore the transition from conventional HiPIMS to mixed-mode by varying the pulse length of the magnetron power supply. The carbon films are characterized using XPS, Raman spectroscopy, ellipsometry, and stress and contact angle measurements. We demonstrate that the presence of arcing is critical for the synthesis of *ta*-C; for shorter pulses where arcing is absent, the sp^3 fraction is very low. We also study the effect of substrate bias, reproducing

the well-known “energy window” effect in which the sp^3 fraction is maximal for a bias of approximately 100 V.³⁰ Together, these two data sets confirm that ta -C can be synthesized with a magnetron sputtering source and demonstrate that an ionized flux produced by arcing is the source of the high sp^3 fraction and associated properties. The full spectrum of amorphous carbon structures is accessible by varying the magnetron pulse profile and substrate bias voltage, enabling the film properties to be tuned for specific applications.

II. EXPERIMENTAL DETAILS

Films were deposited in an AJA sputtering system using an AJA A330 magnetron source fitted with a 76 mm diameter high-density graphite target of 99.99% purity. The base vacuum of the system was 10^{-5} Pa; during sputtering, Ar was introduced to the chamber and an automatic gate valve was used to regulate the pressure to 0.3 Pa. A RUP7 (GBS Elektronik, Dresden) power supply was used to drive the magnetron with one of the five different pulse lengths (90, 120, 150, 180, and 210 μ s) at a rate of 100 Hz. The power supply current was measured using the power supply’s built-in Hall effect current transducer (LEM LF-1005-S). Typical current traces are shown in Figure 1. The charging voltage used was 720 V, except for the case of the longest pulse length (210 μ s) where 640 V was used to avoid triggering the current limit of the power supply. Samples were deposited on (100) silicon substrates positioned 220 mm from the magnetron target surface. The deposition time was 60 min, resulting in films with thicknesses between 25 and 100 nm. The deposition rate as a function of pulse length and substrate bias is shown in Figure 2.

XPS was carried out using an Al K_{α} X-ray source. The resulting spectra were fitted, using the program CasaXPS, with a Shirley background, Gaussian-Lorentzian product line shapes at 285.2 ± 0.1 eV and 284.4 ± 0.1 eV corresponding to sp^3 and sp^2 -hybridized carbon, and two smaller peaks corresponding to carbon-oxygen bonding.³¹ The optical constants and thicknesses of the films were determined using variable angle spectroscopic ellipsometry. Spectroscopic scans over the wavelength range 192.5–1000 nm were collected at incident angles of 60, 65, and 70°. A Cauchy dispersion model

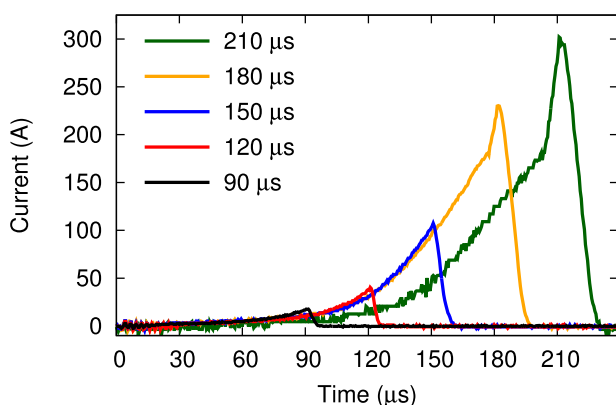


FIG. 1. Evolution of the magnetron current during HiPIMS pulses of various lengths. The power supply charging voltage was 720 V, except for the 210 μ s pulse where a lower value of 640 V was used. The change in slope preceding the maximum of the 180 and 210 μ s traces corresponds to the ignition of an arc.

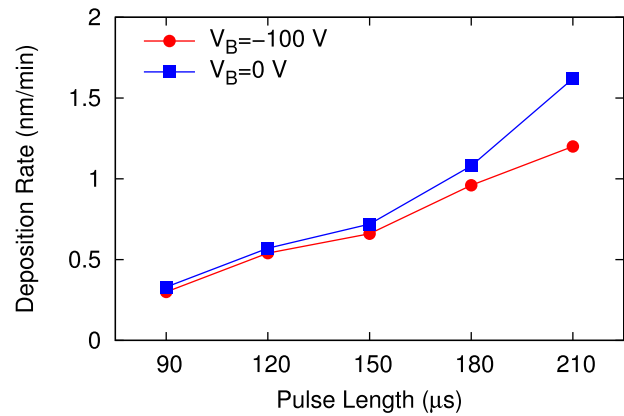


FIG. 2. Deposition rate as a function of pulse length and substrate bias. Film thicknesses were determined by ellipsometry as described in the text.

was used to fit the data and extract the refractive index and extinction coefficient. The thickness determined by ellipsometry was also confirmed by stylus profiler step measurements. Raman spectra were measured using a 514.5 nm excitation laser and fitted with a Breit-Wigner-Fano (BWF) asymmetric Lorentzian lineshape to obtain the fitting parameter Q , which quantifies the asymmetry of the peak.

The intrinsic compressive stress in the films was measured by using a profilometer to measure the wafer curvature and applying Stoney’s equation.³² Contact angle measurements were taken using a drop shape analyser using 45 μ l drops of water and diiodomethane; the surface energy was then obtained using Young’s equation. Hydrogen content was measured by elastic forward recoil detection analysis (ERDA) on a 2 MV tandem ion accelerator, and the total H content was calculated relative to Kapton, which has a H content of 24 at.%. The films were imaged with a Dimension 3100 atomic force microscope (AFM) operating in the tapping mode. These data were analysed using the Gwyddion software package to compute root-mean-square roughness values. Nanoindentation measurements were carried out with a Hysitron instrument fitted with a Berkovich indenter. The film was indented with a maximum force of 200 μ N, producing indents of a depth of less than 10 nm. The load-displacement data were analyzed to determine the reduced modulus by fitting the Hertzian equation to the initial portion of the loading curve as described in Ref. 33. This method was used because the very high elastic recovery of the films meant that the Oliver-Pharr method³⁴ was not appropriate.

III. RESULTS

Our results are presented in two parts. First, we present characterization of films deposited using mixed-mode deposition with a comparatively long pulse length. As shown in our earlier Letter,²⁸ this manner of deposition, combined with a substrate bias of -100 V, results in the synthesis of ta -C. Here, we provide further detail on the underlying data and their analysis and also present new information on hydrogen content and mechanical properties. Additionally, we demonstrate that there is an ion energy window that is optimal for producing ta -C. In the second part of the results section, we vary the HiPIMS pulse length and so transit from

a pure HiPIMS discharge to mixed-mode conditions. The role of ions in the deposition flux is studied by depositing films under conditions of zero and -100 V substrate bias, and characterization is performed on bulk and surface properties.

A. Mixed-mode deposition

Figure 3 shows the XPS spectrum for a *ta*-C film prepared with a pulse length of $210 \mu\text{s}$, which results in an arc igniting during every pulse. The substrate bias was -100 V. The XPS spectrum is fitted by a large peak at 285.2 eV corresponding to sp^3 bonding, a smaller peak at 284.4 eV corresponding to sp^2 bonding, and smaller peaks associated with carbon-oxygen bonds, likely due to surface contamination. The sp^3 fraction inferred from the fit is 81%, very similar to the values reported in our recent work²⁸ in which EELS measurements of the K-edge gave a value of 79%. This agreement demonstrates that for these samples XPS is a reliable means of determining the sp^3 fraction.

Figure 4 shows data obtained via ellipsometry for the same film as examined in Figure 3. Panel (a) shows the wavelength dependence of the refractive index n and extinction coefficient k as obtained from the fitted model. The latter is small across most of the visible spectrum ($k = 6 \times 10^{-5}$ at 550 nm), consistent with the transparent appearance of the films. Panel (b) shows a Tauc plot in which the quantity $\sqrt{\alpha E}$, where $\alpha = 4\pi k/\lambda$ is the absorption coefficient, is plotted as a function of the photon energy E . A linear fit to the data above 3.5 eV yields a Tauc optical gap of 2.66 eV, comparable to literature values⁷ for *ta*-C. At lower energies, $\sqrt{\alpha E}$ falls away quickly, indicating relatively few tail states in the gap.

The hydrogen content of the film examined in Fig. 3 was measured using ERDA. The very low value obtained, 0.3 at. %, demonstrates that the high sp^3 fraction is indicative of *ta*-C, rather than any passivation due to hydrogen. This result is supported by nanoindentation measurements (Fig. 5), which yielded a reduced modulus of 345 GPa. This value is very similar to recent measurements³³ of *ta*-C deposited using a filtered-cathodic-arc for which a value of 360 GPa was obtained using the same equipment and analysis methodology. The load-unload characteristic in Fig. 5 shows that after indentation, the film recovered from the elastic deformation

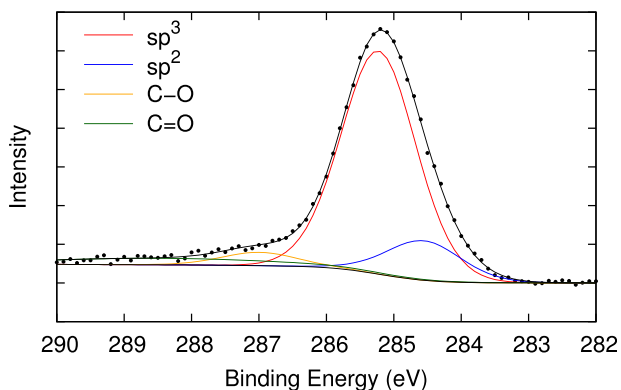


FIG. 3. XPS spectrum for a *ta*-C film deposited with a pulse length of $210 \mu\text{s}$ and a substrate bias of -100 V. The experimental data are shown as black points; the black line is the sum of the fitted components.

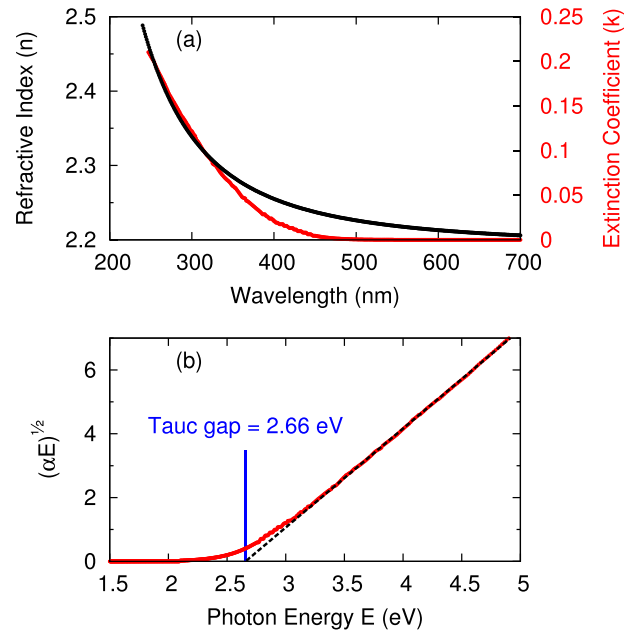


FIG. 4. Ellipsometry-derived data for the same *ta*-C sample as presented in Figure 3. (a) Refractive index (black) and extinction coefficient (red) obtained from the fitted model described in the text. (b) Tauc plot of the optical gap obtained using the extinction coefficient.

completely and no residual indent impression remained. This type of elastic behaviour is typical of *ta*-C.^{33,35,36}

The highly sp^3 bonded film examined in Figures 3 and 4 was deposited with a substrate bias of -100 V. For Figure 6, the substrate bias was varied, with the other deposition parameters held at similar values ($200 \mu\text{s}$, 660 V, 80 Hz, 19 cm) to those used elsewhere in this work. The sp^3 fraction, as measured by XPS, exhibits the characteristic energy window effect seen in ion beam studies of carbon coatings in which the sp^3 fraction is maximal for a bias around -100 V and declines substantially at higher and lower values. Even in the absence of other evidence, this result demonstrates that the deposition flux contains a large fraction of carbon ions.

B. Varying the pulse length

By varying the pulse length, the discharge can be operated in a pure HiPIMS mode and in a mixed-mode. As seen earlier in Figure 1, pulses shorter than $150 \mu\text{s}$ do not trigger

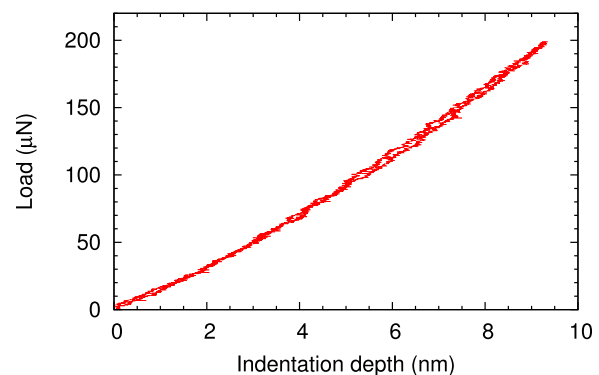


FIG. 5. Force vs displacement curve for a load/unload cycle using a Berkovich indenter on the same *ta*-C sample presented in Figure 3. The data shown are an average of four indents.

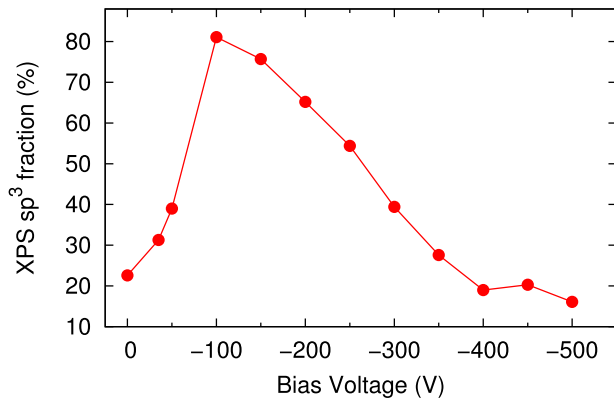


FIG. 6. The sp^3 fraction as determined by XPS of carbon films as a function of substrate bias voltage. The pulse length chosen ($200 \mu\text{s}$) corresponds to mixed-mode deposition.

arcs, whereas longer pulses trigger increasingly longer arcs, moving further into the mixed-mode regime as the pulse length increases. For intermediate pulse lengths, arcs trigger only on some pulses: no arc ignited during the typical $150 \mu\text{s}$ pulse shown, but occasional arcs were observed at this pulse length.

Figures 7 and 8 show XPS and Raman spectra for samples deposited with five different pulse lengths. The other deposition conditions were the same as those used to deposit the samples examined in Figures 3 and 4.

In Figure 7, a pronounced shift can be seen in the position of the maximum XPS intensity as the pulse length increases. This shift corresponds to a gradual transition from sp^2 to sp^3 bonding. Fitting of components to the $90 \mu\text{s}$ data shows that the dominant contribution is the peak at 284.4 eV associated with sp^2 bonding, whereas the fitted spectrum for the $210 \mu\text{s}$ sample (already shown in Figure 3) is dominated by the sp^3 peak. The sp^3 fractions for these two cases are 26% and 82%, respectively, determined from the relative areas of the fitted components.

The Raman spectrum (Figure 8) is also strongly dependent on the pulse length and varies in a manner consistent

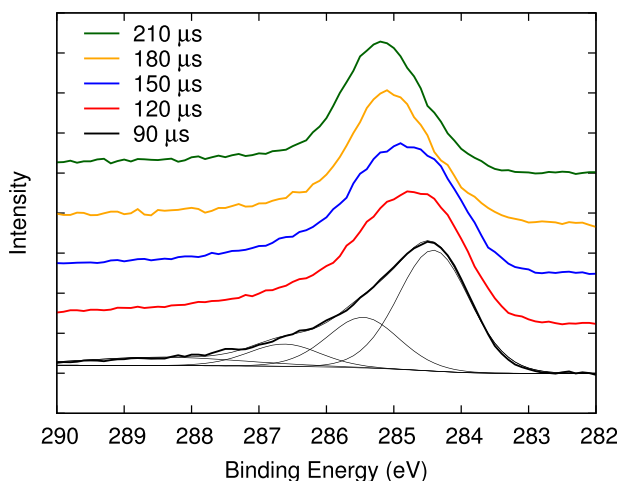


FIG. 7. XPS spectra for carbon films deposited using various pulse lengths as shown in Figure 1. The substrate bias was -100 V . For the film deposited with a $90 \mu\text{s}$ pulse length, the fitting components used to extract the sp^3 fraction are also shown.

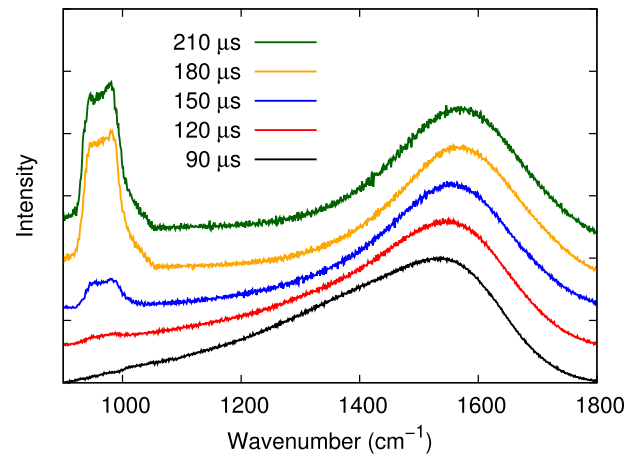


FIG. 8. Raman spectra for carbon films deposited using various pulse lengths as shown in Figure 1. The substrate bias was -100 V .

with the sp^3 fractions determined by XPS. For short pulse lengths, the peak around 1550 cm^{-1} is highly asymmetric, consistent with an amorphous carbon with a low sp^3 fraction. With increasing pulse length (and sp^3 fraction), this peak becomes increasingly symmetric. The square-topped feature around 950 cm^{-1} is a second-order peak of the silicon substrate.³⁷ It becomes more prominent at longer pulse lengths where the carbon films are more transparent.

Figure 9 shows the dependence on pulse length of the film sp^3 fraction, Tauc gap, Raman Q asymmetry coefficient, and film stress for substrate bias voltages of -100 and 0 V . The -100 V data for the sp^3 fraction and the Raman Q coefficient were extracted from the spectra shown in Figures 7 and 8. Each of the four quantities plotted reflects the tetrahedral character of the film: a $ta\text{-C}$ film will have a high sp^3 fraction, a Tauc gap approaching 3 eV ,⁷ a symmetric Raman peak, typically with a Q fitting parameter approaching -20 ,³⁷ and a film stress of above 6 GPa .³⁸

The samples deposited at -100 V bias show a monotonic increase in each quantity with the pulse length. A jump in each quantity occurs between the 150 and $180 \mu\text{s}$ samples, corresponding to the onset of mixed-mode operation, and the samples deposited with pulse lengths of 180 and $210 \mu\text{s}$ meet the criteria for $ta\text{-C}$. In contrast, at 0 V bias, all four quantities have little if any dependence on the pulse length, and none of these samples exhibit a tetrahedral character. This demonstrates that mixed-mode deposition, as opposed to conventional HiPIMS, is necessary for the deposition of $ta\text{-C}$. Further, the fact that $ta\text{-C}$ does not form without a substrate bias, even in the case of mixed-mode deposition, demonstrates that while the mixed-mode discharge is an efficient source of carbon ions, their native energy is insufficient to access the tetrahedral form. This observation explains an aspect of the deposition rate data in Figure 2. For long pulse lengths, the deposition rate is lower when a negative substrate bias is used because the negative bias increases the density of the films, resulting in thinner films for the same incident flux of carbon.

Figures 10(a) and 10(b) show surface energy and contact angle data for the sample set examined in Figure 9. The 0 V films show little variation in their properties as the pulse length is varied. Using -100 V bias, the surface

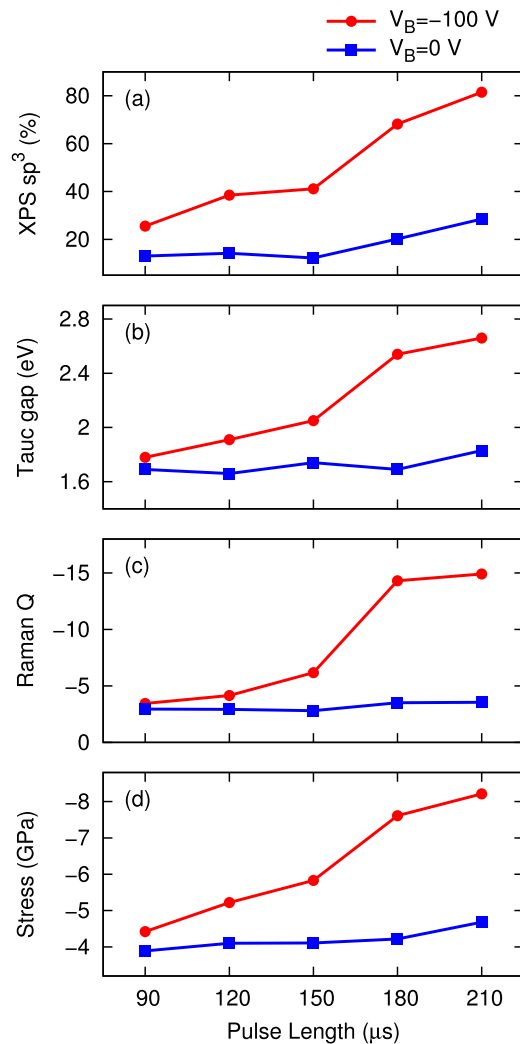


FIG. 9. Bulk properties of carbon films as a function of pulse length for two different substrate biases. Films with high diamond-like character are obtained only with pulse lengths of 180 or 210 μs and a substrate bias of -100 V. (a) sp^3 fraction determined by XPS; (b) Tauc gap determined using ellipsometry; (c) fitting parameter Q quantifying the asymmetry of the Raman spectrum; (d) compressive stress determined by substrate curvature.

becomes increasingly hydrophobic as the pulse length increases. The data for the most tetrahedral film (210 μs and -100 V) compare well with literature values of $75\text{--}80^\circ$ for the *ta*-C water contact angle^{39,40} and 43 mN/m for the *ta*-C surface energy.³⁹

The roughness values of the samples as measured with atomic force microscopy are shown in Figure 10(c). The films become slightly smoother with increasing pulse length, and the films deposited at -100 V have a roughness 0.15 nm less than those deposited at 0 V. The two most tetrahedrally bonded films (-100 V, 180 and 210 μs) have roughness values of 0.11 nm, essentially the same as the literature value for *ta*-C of ~ 0.12 nm as measured by Casiraghi *et al.*⁴¹

IV. DISCUSSION AND CONCLUSION

Our recent study of mixed-mode HiPIMS deposition²⁸ showed that tetrahedral amorphous carbon can be synthesized using a magnetron sputtering apparatus. In that work, the

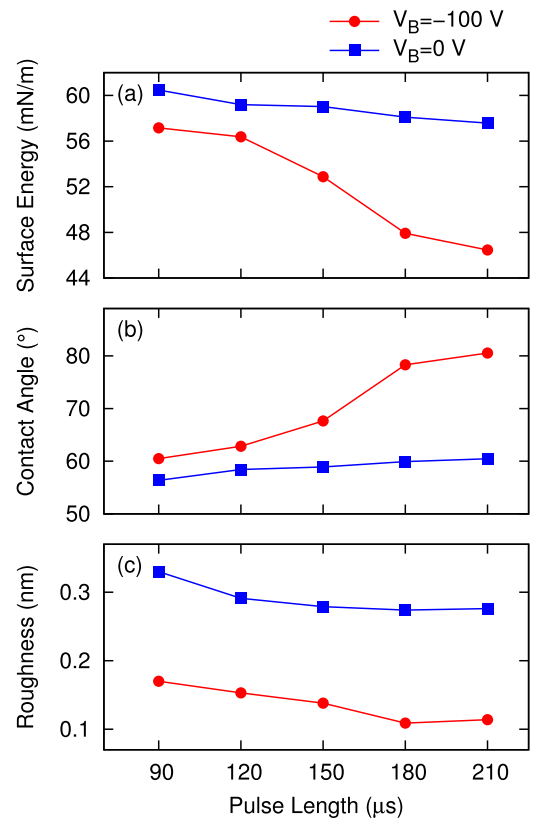


FIG. 10. Surface properties of carbon films as a function of pulse length for two different substrate biases; (a) surface energy, (b) water contact angle, and (c) AFM roughness. As described in the text, the data for the film deposited with a pulse length of 210 μs and bias of -100 V are similar to literature values for *ta*-C films.

repeated triggering of short-lived arcs on the target was identified as a significant source of carbon ions. This conclusion was based upon optical emission spectroscopy, visual similarities with cathodic arcs, a minimum average ion energy of 20 eV inferred from the substrate current, and a high sp^3 fraction in deposited films. The Ar pressure was found to be an important deposition parameter, with values above 0.3 Pa resulting in films with low tetrahedral character.

In this work, we examine two other important process parameters: the length of the pulse to the magnetron and the substrate bias voltage. The former indirectly determines the ionized fraction of the deposited species, whereas the substrate bias sets the energy of these ions as they impact the substrate. We also present a comprehensive characterization of the bulk and surface properties of the deposited carbon films, extending upon our earlier work by including data for hydrogen content, hardness, surface energy, and roughness.

The pulse length is an important deposition parameter that controls the ionized fraction of the plasma by determining whether or not mixed-mode deposition occurs. For short pulse lengths, the deposition flux arises from a pure HiPIMS glow discharge, while for pulse lengths longer than 150 μs , an increasing fraction of material is generated by the mixed-mode arcs as shown in Figure 1. The formation of *ta*-C can be definitively attributed to the arc component of mixed-mode operation, since when arcs are not present, the films deposited have low sp^3 content. Furthermore, the reason that

the mixed-mode arcs produce this effect must be a substantially increased ionised fraction of C species in the plasma, because a high film sp^3 content is never obtained in samples deposited without bias, regardless of the pulse length used. The presence of these ions is additionally confirmed in Figure 6 by the appearance of the “energy window” effect typical of PVD *ta*-C deposition processes. These results mean that in mixed-mode deposition, the structure and properties of the deposited film can be tailored by the application of substrate bias in the same manner as is possible with deposition methods using ion beams. Mixed-mode deposition also affords an additional opportunity for control of the film growth as the ionised fraction of the plasma flux can be adjusted by varying the pulse length.

Finally, we note that many previous reports^{17–26} on deposition of carbon using HiPIMS have described films with sp^3 fractions of a maximum of $\sim 45\%$. This result is reproduced in our work for short pulse lengths, where the mixed-mode arcs do not ignite: for pulse lengths of 150 μs or shorter, the maximum sp^3 fraction reached is 41%. For the shortest pulse lengths, where the peak current is smallest, the sp^3 fraction declines further, as the sputtering process becomes closer to the case of a low-current DC magnetron discharge.

In conclusion, we have unambiguously demonstrated that the synthesis of *ta*-C by mixed-mode HiPIMS deposition is due to ionization arising from the arcs appearing at the end of the pulse. When the arcs are suppressed by early termination of the pulse or when the substrate bias voltage is set outside the optimal window, amorphous carbon films of low sp^3 content are produced. This result means that mixed-mode operation provides a carbon deposition flux where the fraction of species ionized is tunable to a high degree. This ability to control the ionized fraction of the deposited species is in addition to the usual ability to tune the energy of deposited ions by manipulation of the substrate bias. Having this extra degree of control opens possibilities for new carbon-based thin film designs. This deposition source could be used to synthesise a wide range of amorphous carbons, including graded coatings and multilayers where the sp^3 fraction is varied either continuously or abruptly during the deposition. Such a source would also be useful in other thin film applications where the presence of energetic ionized carbon species is of benefit such as the deposition of refractory carbides.

ACKNOWLEDGMENTS

The authors gratefully acknowledge support from the Australian Research Council. N.A.M. acknowledges a fellowship under FT120100924. We also thank Mihail Ionescu of the Australian Nuclear Science and Technology Organisation for performing the ERDA measurements.

¹K. Bewilogua and D. Hofmann, *Surf. Coat. Technol.* **242**, 214 (2014).

²J. Vetter, *Surf. Coat. Technol.* **257**, 213 (2014).

³M. Stüber, S. Ulrich, H. Leiste, A. Kratzsch, and H. Holleck, *Surf. Coat. Technol.* **116–119**, 591 (1999).

⁴J. J. Cuomo, J. P. Doyle, J. Bruley, and J. C. Liu, *Appl. Phys. Lett.* **58**, 466 (1991).

⁵D. R. McKenzie, *Rep. Prog. Phys.* **59**, 1611 (1996).

⁶S. Xu, B. K. Tay, H. S. Tan, L. Zhong, Y. Q. Tu, S. R. P. Silva, and W. I. Milne, *J. Appl. Phys.* **79**, 7234 (1996).

⁷M. Chhowalla, J. Robertson, C. W. Chen, S. R. P. Silva, C. A. Davis, G. A. J. Amaratunga, and W. I. Milne, *J. Appl. Phys.* **81**, 139 (1997).

⁸J. Schwan, S. Ulrich, H. Roth, H. Ehrhardt, S. R. P. Silva, J. Robertson, R. Samlenski, and R. Brenning, *J. Appl. Phys.* **79**, 1416 (1996).

⁹F. Bernhardt, K. Georgiadis, L. Dolle, O. Dambon, and F. Klocke, *Mat.-wiss u. Werkstofftech.* **44**, 661 (2013).

¹⁰V. Kouznetsov, K. Macák, J. M. Schneider, U. Helmersson, and I. Petrov, *Surf. Coat. Technol.* **122**, 290 (1999).

¹¹U. Helmersson, M. Lattemann, J. Bohlmark, A. P. Ehiasarian, and J. T. Gudmundsson, *Thin Solid Films* **513**, 1 (2006).

¹²J. Lin, J. J. Moore, W. D. Sproul, B. Mishra, J. A. Rees, Z. Wu, R. Chistyakov, and B. Abraham, *Surf. Coat. Technol.* **203**, 3676 (2009).

¹³A. Anders, *Surf. Coat. Technol.* **205**(Suppl. 2), S1 (2011).

¹⁴J. Gudmundsson, N. Brenning, D. Lundin, and U. Helmersson, *J. Vac. Sci. Technol. A* **30**, 030801 (2012).

¹⁵R. Bandorf, V. Sittinger, and G. Bräuer, “4.04-High Power Impulse Magnetron Sputtering—HIPIMS,” in *Comprehensive Materials Processing* (Elsevier, Oxford, 2014), Vol. 4, pp. 75–99.

¹⁶A. P. Ehiasarian, R. New, W. D. Münz, L. Hultman, U. Helmersson, and V. Kouznetsov, *Vacuum* **65**, 147 (2002).

¹⁷K. Sarakinos, A. Braun, C. Zilkens, S. Mráz, J. M. Schneider, H. Zoubos, and P. Patsalas, *Surf. Coat. Technol.* **206**, 2706 (2012).

¹⁸S. P. Bugaev, V. G. Podkovyrov, K. V. Oskomov, S. V. Smaykina, and N. S. Sochugov, *Thin Solid Films* **389**, 16 (2001).

¹⁹B. M. DeKoven, P. R. Ward, R. E. Weiss, R. A. Christie, W. Scholl, D. Sproul, F. Tomasel, and A. Anders, in *46th Annual Technical Conference Proceedings of the Society of Vacuum Coaters* (2003), p. 158.

²⁰L. A. Donohue, A. Torosyan, P. May, D. E. Wolfe, J. Kulik, and T. J. Eden, *Plat. Surf. Finish.*, March 2009, pp. 38–46.

²¹S. Nakao, K. Yukimura, H. Ogiso, S. Nakano, and T. Sonoda, *Vacuum* **89**, 261 (2013).

²²M. Hiratsuka, A. Azuma, H. Nakamori, Y. Kogo, and K. Yukimura, *Surf. Coat. Technol.* **229**, 46 (2013).

²³K. Yukimura, H. Ogiso, S. Nakano, S. Nakao, and K. Takaki, *IEEE Trans. Plasma Sci.* **41**, 3012 (2013).

²⁴M. Huang, X. Zhang, P. Ke, and A. Wang, *Appl. Surf. Sci.* **283**, 321 (2013).

²⁵J. Lin, W. D. Sproul, R. Wei, and R. Chistyakov, *Surf. Coat. Technol.* **258**, 1212 (2014).

²⁶T. Konishi, K. Yukimura, and K. Takaki, *Surf. Coat. Technol.* **286**, 239 (2016).

²⁷M. Lattemann, A. Moafi, M. M. M. Bilek, D. G. McCulloch, and D. R. McKenzie, *Carbon* **48**, 918 (2010).

²⁸R. Ganesan, D. G. McCulloch, N. A. Marks, M. D. Tucker, J. G. Partridge, M. M. M. Bilek, and D. R. McKenzie, *J. Phys. D* **48**, 442001 (2015).

²⁹M. Lattemann, B. Abendroth, A. Moafi, D. G. McCulloch, and D. R. McKenzie, *Diamond Relat. Mater.* **20**, 68 (2011).

³⁰P. J. Fallon, V. S. Veerasamy, C. A. Davis, J. Robertson, G. A. J. Amaratunga, W. I. Milne, and J. Koskinen, *Phys. Rev. B* **48**, 4777 (1993).

³¹J. Díaz, G. Paolicelli, S. Ferrer, and F. Comin, *Phys. Rev. B* **54**, 8064 (1996).

³²G. S. Stoney, *Proc. R. Soc. A* **82**, 172 (1909).

³³M. Kracica, C. Kocer, D. W. M. Lau, J. G. Partridge, J. E. Bradby, B. Haberl, D. R. McKenzie, and D. G. McCulloch, *Carbon* **98**, 391 (2016).

³⁴W. Oliver and G. Pharr, *J. Mater. Res.* **19**, 3 (2004).

³⁵C. A. Charitidis, *Int. J. Refract. Met. Hard Mater.* **28**, 51 (2010).

³⁶J. M. Jungk, B. L. Boyce, T. E. Buchheit, T. A. Friedmann, D. Yang, and W. W. Gerberich, *Acta Mater.* **54**, 4043 (2006).

³⁷S. Praver, K. W. Nugent, Y. Lifshitz, G. D. Lempert, E. Grossman, J. Kulik, I. Avigal, and R. Kalish, *Diamond Relat. Mater.* **5**, 433 (1996).

³⁸D. W. M. Lau, D. G. McCulloch, M. B. Taylor, J. G. Partridge, D. R. McKenzie, N. A. Marks, E. H. T. Teo, and B. K. Tay, *Phys. Rev. Lett.* **100**, 176101 (2008).

³⁹J. S. Chen, S. P. Lau, Z. Sun, G. Y. Chen, Y. J. Li, B. K. Tay, and J. W. Chai, *Thin Solid Films* **398–399**, 110 (2001).

⁴⁰H. Han, F. Ryan, and M. McClure, *Surf. Coat. Technol.* **120–121**, 579 (1999).

⁴¹C. Casiraghi, A. C. Ferrari, R. Ohr, A. J. Flewitt, D. P. Chu, and J. Robertson, *Phys. Rev. Lett.* **91**, 226104 (2003).